p-^{3}He and p-^{3}H Angular Correlations from the Reaction D(^{3}He, p)[†]

Wen-Kuan Lin* and F. Scheibling*

California Institute of Technology, Pasadena, California 91109

(Received 26 January 1970)

Protons emitted from the bombardment of deuterium with a 16.5-MeV ^{3}He beam have been measured at $\theta_p = 30°$, in coincidence with the other charged particles from the reaction. Angular correlations at $6.6 \leqslant E_p \leqslant 7.8$ MeV have been obtained and compared with a modified-Born-approximation calculation of the ^{3}He stripping. The angle-energy correlation and the p-^{3}H to p-^{3}He branching ratio can be reproduced if the ^{3}H+p phase shifts of Meyerhof and McElearney and the ^{3}He+n phase shifts of Bransden, Robertson, and Swan are used to describe the respective interactions in the final states. In agreement with Barit *et al.*, the triplet s-wave ^{3}He+n phase shifts are found to be negative.

I. INTRODUCTION

The three-body breakups from the ^{3}He + D reaction into $p + ^3$He + n and $p + ^3$H + p have been reported from measurements of single-proton energy spectra[1] and charged-particle coincidences.[2,3] The results have been interpreted in terms of two ^{4}He excited states near 20 and 21.2 MeV. Analyses[4,5] of final-state interactions have shown that the 20-MeV state is identical with the 0^+ resonance found by Werntz,[6] and that the 21.2-MeV state is consistent with a p-wave final-state interaction in the $p + ^3$H system.

The present work was undertaken to study the effects of these final-state interactions on the angular correlations; in particular, for ^{4}He excitation energies near 21 MeV. From the viewpoint of studying reaction mechanisms, Yu and Meyerhof[5] have analyzed the single-proton energy spectra and also the single-neutron energy spectra[7,8] from the mirror reaction ^{3}H(d, n) with a modified-Born-approximation calculation. They have found that the singles spectra cannot distinguish between different breakup modes, and suggested the use of coincidence requirements.

In our measurements at $E_T = 16.5$ MeV, $\theta_p = 30°$ and 6.6 MeV $\leqslant E_p \leqslant 8.6$ MeV, we have found that the p-^{3}He and p-^{3}H angular correlations, from D-(^{3}He, p), have an axis of symmetry along the recoil direction of the ^{4}He system. As will be discussed in Sec. III, this suggests that ^{3}He stripping is the predominant mechanism. For this mechanism, it was found possible to reproduce the correlation data using the ^{3}He + n phase shifts of Bransden, Robertson, and Swan[9] and the ^{3}H + p phase shifts of Meyerhof and McElearney[10] to represent the respective final-state interactions. In agreement with the results of a charge-invariant analysis,[11] the triplet s-wave ^{3}He + n phase shifts are found to be negative.

II. EXPERIMENTAL METHOD

The cross section of a three-body reaction, $1 + 2 \to 3 + 4 + 5$, is related to the transition matrix element T_{fi} by

$$\Delta\sigma = \frac{2\pi}{\hbar v_{12}} \frac{1}{(2\pi\hbar)^6} \int_{\Delta\tau} \langle |T_{fi}|^2 \rangle \delta(\vec{P}_1 + \vec{P}_2 - \vec{P}_3 - \vec{P}_4 - \vec{P}_5)$$
$$\times \delta\left(\frac{P_1^2}{2m_1} + \frac{P_2^2}{2m_2} + Q - \frac{P_3^2}{2m_3} - \frac{P_4^2}{2m_4} - \frac{P_5^2}{2m_5}\right) d\vec{P}_3 d\vec{P}_4 d\vec{P}_5 ,$$

$$(1)$$

where v_{12} is the relative velocity of particles 1 and 2, Q is the Q value of the reaction, and $\langle |T_{fi}|^2 \rangle$ is the squared modulus of the transition matrix element, averaging and summing over the initial- and final-state spin projections. Integrations are to be carried over the volume of the phase-space region $\Delta\tau$ determined by the angle and energy resolutions of the detectors. In the laboratory system, the target deuteron (particle 1) is at rest, and the integration in Eq. (1) yields the cross section for the coincident detection of particles 3 and 4:

$$\Delta\sigma = \frac{2\pi m_2}{\hbar P_2} \frac{1}{(2\pi\hbar)^6} \Delta E_3 \Delta\Omega_3 \Delta\Omega_4 m_3 P_3 \langle |T_{fi}|^2 \rangle$$
$$\times \frac{P_4^2}{|P_4/m_{45} - (\hat{P}_4/m_5) \cdot (\vec{P}_2 - \vec{P}_3)|} .$$

$$(2)$$

Here $\Delta\Omega_i$ and ΔE_i are the angle and energy resolutions of the detector that particle i enters, and m_{jk} is the reduced mass of particle j with respect to particle k. The detector that particle 4 enters is set to detect particles with all the energies allowed by kinematics. In terms of the relative momentum of pair (4 + 5), i.e., $\vec{q}_{45} = m_{45}[\vec{P}_4(1/m_4) - \vec{P}_5(1/m_5)]$, Eq. (1) can also be integrated as

$$\Delta\sigma = \frac{2\pi m_2}{\hbar P_2} \frac{1}{(2\pi\hbar)^6} \Delta E_3 \Delta\Omega_3 \Delta\Omega_{45} m_3 P_3 \langle |T_{fi}|^2 \rangle m_{45} q_{45} ,$$

$$(3)$$

where $\Delta\Omega_{45}$ is the angular resolution $\Delta\Omega_4$ seen in the recoil-center-of-mass (rcm) system of the pair (4+5). The ratio $\Delta\Omega_4/\Delta\Omega_{45}$, which will be used in the transformation of differential cross sections from the laboratory system to the rcm system, is obtained directly by transformation of the solid angle or by equating Eqs. (2) and (3). Since particles 5 and 4 are emitted oppositely in their rcm system, the angular correlation between particles 3 and 5 can be reduced to that between particles 3 and 4. Particle 4 is then taken as either ^{3}H or ^{3}He.

The incident 16.5-MeV ^{3}He beam was obtained from the Office of Naval Research–California Institute of Technology tandem accelerator, magnetically analyzed and collimated to a 1.5-mm square before striking the target. The target (~0.25 mg/cm^2) was prepared from deuterated dotriacontane [$CD_3(CD_2)_{30}CD_3$ of 99.7 at.% in D], which was dissolved in carbon tetrachloride and allowed to dry on a copper-foil backing (~50 μg/cm^2). The protons (particles 3), detected at 30°, were analyzed by a 61-cm magnetic spectrometer. The $\Delta\theta$ and $\Delta\Phi$ acceptance angles of the spectrometer were set at 1 and 4°, respectively. Particles traversing the spectrometer were detected by a surface-barrier counter located in the focal plane; a slit just in front of the counter defined an energy window of $\Delta E_3 = E_3/90$. A 0.25-mm aluminum sheet was
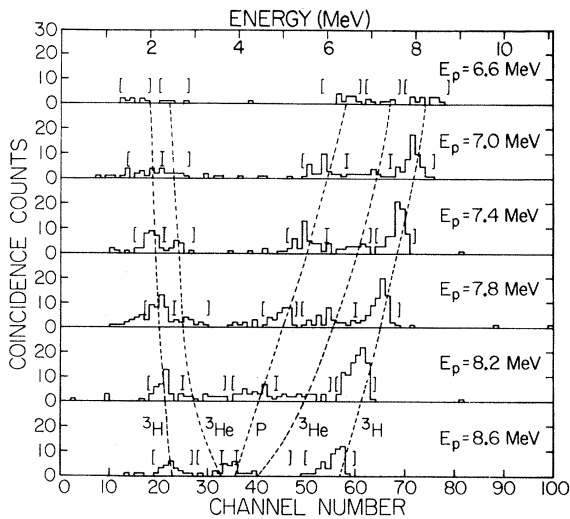
placed in front of the counter to stop the α particles which arrive with the same energy as the protons. Other charged particles from the reaction were detected in coincidence with the protons by a surface-barrier counter in the target chamber, at negative angles ranging from 10 to 60°. The $\Delta\theta$ and $\Delta\Phi$ acceptance angles of this counter were, respectively, 2 and 8°. Coincidence requirements were imposed in circuitry with a resolving time of 110 nsec. Some of the coincidence spectra obtained are shown in Figs. 1 and 2. After each of the coincidence runs, a singles spectrum was taken to facilitate correction for random coincidences, which were always less than 10%.

The coincidence yield is related to the differential cross section by

$$Y_{\text{coin}} = \frac{d^3\sigma}{dE_3 d\Omega_3 d\Omega_4} \Delta E_3 \Delta\Omega_3 \Delta\Omega_4 N_d N_T , \qquad (4)$$

where N_d is the number of deuterium atoms per unit area of the target, and N_T is the total number of incident ^{3}He particles striking the target. The proton yield in singles spectra from the spectrometer in the same run, i.e.,

$$Y_{\text{sp}} = \left[\left(\frac{d^2\sigma}{dE_3 d\Omega_3} + \frac{d^2\sigma_C}{dE_3 d\Omega_3}\frac{N_C}{N_d}\right)\right]\Delta E_3 \Delta\Omega_3 N_d N_T , \qquad (5)$$
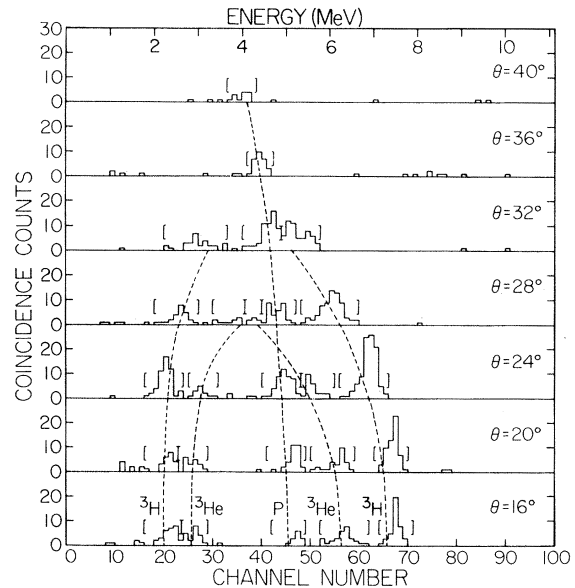

FIG. 1. Coincidence spectra from D(^{3}He,p) at E_T =16.5 MeV. Protons of the energies indicated were detected at 30° in the magnetic spectrometer, whose resolutions were set at $\Delta E/E = 1.11\%$, $\Delta\theta = 1°$, and $\Delta\Phi = 4°$. The acceptance angles for the counter, fixed at −20° to the beam, in the target chamber were 2 and 8° along the θ and Φ directions. The coincidence resolving time was 110 nsec. The dashed lines are drawn from the three-body kinematics, and the parentheses define regions where the coincidence counts are summed.

FIG. 2. Coincidence spectra from D(^{3}He,p) at E_T =16.5 MeV. The 7.8-MeV protons were detected at 30° in the magnetic spectrometer with $\Delta E/E = 1.11\%$, $\Delta\theta = 1°$, and $\Delta\Phi = 4°$. The acceptance angles for the counter, set at the negative angles indicated, in the target chamber were 2 and 8°, respectively, along θ and Φ directions. The coincidence resolving time was 110 nsec. The dashed lines are the three-body kinematics, and the parentheses define the regions where the coincidence counts are summed.

was used as a measure of $N_d \times N_T$. The contributions to the proton yield from carbon are included in the term $N_C \times d^2\sigma_C/dE_3 d\Omega_3$. Here N_C is the number of carbon atoms per unit area of the target. In order to normalize the spectra taken at different E_3, a second surface-barrier counter was set in the target chamber ($60°$ to the beam axis) during the last day of this experiment to monitor the elastic deuterons from D(^{3}He, d). The number of protons counted by the spectrometer, normalized to 10 counts of these deuterons, is denoted by $N(E_3)$ and is plotted in Fig. 3 as a function of proton energy. Since $N(E_3)$ is proportional to the quantity appearing within the squared brackets of Eq. (5), the quantity $Y_{sp}/N(E_3)$ was used to determine the differential cross section from Y_{coin}. The uncertainty in this normalization due to possible target deterioration during the runs was found to be less than 10%.

The differential cross section transformed to the rcm system of particles 4 and 5 is shown in Fig. 4, where the recoil-^{4}He direction ($\vec{P}_2 - \vec{P}_3$) was chosen as an axis of reference. The quantity ξ plotted is the following, with the constant C chosen arbitrarily equal to 0.0796:

$$\xi = C \times \frac{90}{E_3} \times N(E_3) \times \frac{Y_{coin}}{Y_{sp}} \times \frac{\Delta\Omega_4}{\Delta\Omega_{45}}$$

$$= const \times \frac{d^3\sigma}{dE_3 d\Omega_3 d\Omega_{45}} . \qquad (6)$$

Here, from Eq. (3), the differential cross section in the rcm system is

$$\frac{d^3\sigma}{dE_3 d\Omega_3 d\Omega_{45}} = \frac{2\pi m_2}{\hbar P_2} \frac{1}{(2\pi\hbar)^6} \langle |T_{fi}|^2 \rangle m_3 P_3 m_{45} q_{45} . \qquad (7)$$

Both ^{3}He and ^{3}H are found to be emitted symmetrically with respect to the ^{4}He recoil direction. The relative energy of the pair (4+3) is always higher than that of (4+5), and the final-state inter-
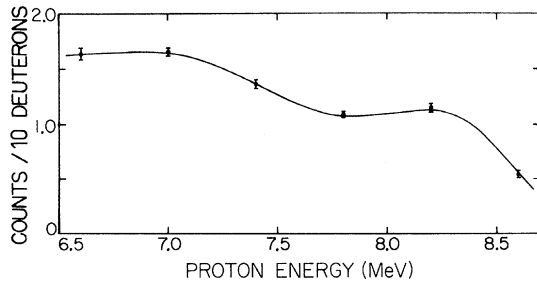

FIG. 3. Proton yield in singles spectra measured in the magnetic spectrometer at $30°$. The number of protons counted by the spectrometer ($\Delta E/E = 1.11\%$, $\Delta\theta = 1°$, and $\Delta\Phi = 4°$) was normalized to 10 elastic deuterons from D(^{3}He, d), measured by a surface-barrier counter at $60°$ in the target chamber. This ratio is denoted by $N(E_3)$ in the text and was used in data reduction [see Eq. (6)].

action is stronger for lower relative energy, hence the contribution due to the (4+3) final-state interaction is expected to be smaller. For the pair (3+5), i.e., the two-nucleon system, the relative energy may become quite low around $(\theta_4)_{lab} \sim -30°$ or $(\theta_4)_{rcm} \sim -70°$; however, no enhancement in the angular correlation, due to $p+n$ or $p+p$ final-state interactions, was seen.

III. MODIFIED-BORN-APPROXIMATION CALCULATION

Because no definite enhancement due to a two-nucleon final-state interaction was seen, the reaction in this phase-space region, according to Yu and Meyerhof,[5] may proceed through the following mechanisms:

A (D) ^{3}He picks up a neutron from the target deuteron and forms a ^{3}H$+p$ (^{3}He$+n$) interacting pair.

B (E) ^{3}He strips its deuteron to the target deuteron to form a ^{3}H$+p$ (^{3}He$+n$) interacting pair.

C (F) ^{3}He breaks up giving one neutron (proton) to the target deuteron, and the ^{3}H (^{3}He) formed then interacts with the other proton (neutron) from the breakup.

G ^{3}He interacts with the neutron from direct breakup of the target deuteron.

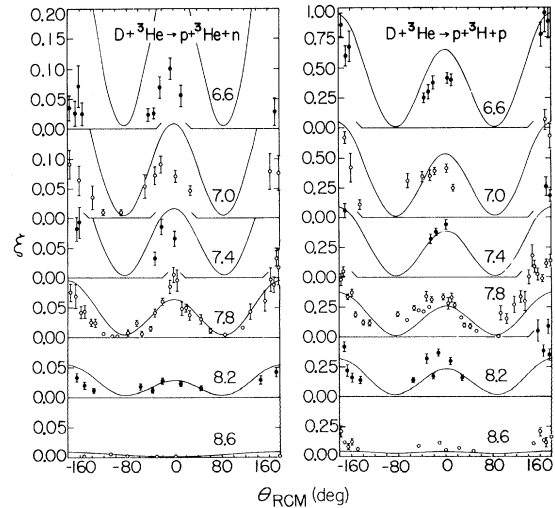FIG. 4. Energy and angle correlation from D(^{3}He,p) at $E_T = 16.5$ MeV. The coincidence counts of the peaks under the kinematic lines are converted, according to Eq. (6), to the rcm system of the recoiled ^{4}He. The recoil direction was used as axis of reference. Errors in quantity ξ plotted include the statistical error, uncertainties in random correction and in assignments of counts to different groups of particles. The curves, labeled with the proton energy, are the modified-Born-approximation; see text for the parameters involved.

From a modified-Born-approximation calculation including only a Wigner nucleon-nucleon force, the transition matrix element for each of these mechanisms has also been given. The predicted angular correlation has an axis of symmetry along the momentum transfer to the relative motion of the final-state interacting pair of particles. For $E_T = 16.5$ MeV, $E_p = 7.8$ MeV, and $\theta_p = 30°$, the angle θ between the momentum transfer and the beam axis, and the relative amplitude[12] of forming the final-state interacting pair are calculated for each mechanism as:

Mechanism	θ (deg)	Amplitude $l=0$	$l=1$
A (D)	16.3	-0.72×10^{-4}	-1.58×10^{-4}
B (E)	-16.8	1.00	1.03
C (F)	-4.0	1.03×10^{-8}	3.45×10^{-8}
G	-14.4	-55	-8.9

As observed, the symmetry axis of the angular correlations lay along the ^{4}He recoil direction, and was also at $-16.8°$ to the beam axis. The mechanisms A (D) and C (F) therefore could be neglected on account of the θ's and the smallness of their relative amplitudes.

When the angular correlations at $E_p = 7.8$ MeV were analyzed by a least-squares fit to Legendre polynomials, the branching ratio of p-^{3}H to p-^{3}He was found to be 7.91 ± 0.63. In order to predict this ratio, it is clear that one could not include the mechanism G, because it does not lead to the p-^{3}H branch. The mechanism G also underestimates the p-wave contribution. We therefore proceed, in the following, to a detailed calculation of mechanism B (E), including exchange forces, as well as the Wigner force in the nucleon-nucleon interaction. If one labels the nucleons in the target deuteron by 1 and 2, and those in the incident ^{3}He by 3, 4, and 5, the initial- and final-state wave functions corresponding to mechanism B (E) can be written as

$$\Psi_i = \phi(\vec{r}_1, \vec{r}_2)\psi(\vec{r}_3, \vec{r}_4, \vec{r}_5)\exp\left\{i\vec{K}_T\cdot\left[\tfrac{1}{3}(\vec{r}_3+\vec{r}_4+\vec{r}_5) - \tfrac{1}{2}(\vec{r}_1+\vec{r}_2)\right]\right\},$$

and

$$\Psi_f = \psi(\vec{r}_1, \vec{r}_2, \vec{r}_3)\chi(4)\chi_4'[\vec{r}_4 - \tfrac{1}{3}(\vec{r}_1+\vec{r}_2+\vec{r}_3)]\chi(5)\exp\left\{i\vec{K}_p\cdot[\vec{r}_5 - \tfrac{1}{4}(\vec{r}_1+\vec{r}_2+\vec{r}_3+\vec{r}_4)]\right\},$$

where $\hbar\vec{K}_T$ ($\hbar\vec{K}_p$) is the momentum of the initial-state ^{3}He (final-state proton) in the c.m. system. χ_4' describes the relative motion of the final-state interacting pair consisting of a nucleon and a three-nucleon nucleus. χ, ϕ, and ψ are the internal wave functions of the one-, two-, and three-nucleon systems, respectively. They are assumed to be separable in space and spin-isospin variables, and are taken as:

(1) Nucleon

$$\chi(1) = \rho_1^{m_1}\eta_1^{\mu_1},$$

where ρ, η are the spin and isospin matrices.

(2) Two-nucleon nucleus (i.e., deuteron)

$$\phi(\vec{r}_1, \vec{r}_2) = D^{M_d,0}(1, 2)\left(\frac{2\alpha^2}{\pi}\right)^{3/4} e^{-\alpha^2|\vec{r}_1-\vec{r}_2|^2},$$

where

$$D^{M_d,0}(1, 2) = \sum_{m_1 m_2}\sum_{\mu_1\mu_2}(\tfrac{1}{2}\tfrac{1}{2}m_1 m_2|1M_d)(\tfrac{1}{2}\tfrac{1}{2}\mu_1\mu_2|00)\rho_1^{m_1}\rho_2^{m_2}\eta_1^{\mu_1}\eta_2^{\mu_2}.$$

(3) Three-nucleon nucleus[13]

$$\psi(\vec{r}_1, \vec{r}_2, \vec{r}_3) = R^{n\,\nu}(1, 2, 3)\left(\frac{3}{\pi^2}\right)^{3/4}\gamma^3\exp\left\{-\gamma^2\left[\tfrac{3}{4}|\vec{r}_1-\vec{r}_2|^2 + |\vec{r}_3 - \tfrac{1}{2}(\vec{r}_1+\vec{r}_2)|^2\right]\right\},$$

where

$$R^{n\,\nu}(1, 2, 3) = \frac{1}{\sqrt{6}}\sum_{m_1 m_2}\sum_{\mu_1\mu_2}(\tfrac{1}{2}\tfrac{1}{2}m_1 m_2|00)(\tfrac{1}{2}\tfrac{1}{2}\mu_1\mu_2|00)[\rho_1^{m_1}\rho_2^{m_2}\rho_3^n(\eta_1^{\mu_1}\eta_2^\nu + \eta_1^\nu\eta_2^{\mu_1})\eta_3^{\mu_2} - (\rho_1^{m_1}\rho_2^n + \rho_1^n\rho_2^{m_1})\rho_3^{m_2}\eta_1^{\mu_1}\eta_2^{\mu_2}\eta_3^\nu].$$

The inverse decay lengths for the bound wave functions are taken from Ref. 5 as $\alpha = 0.167$ F^{-1} and $\gamma = 0.36$ F^{-1}. The interaction responsible for the mechanisms B (E) is $V = V_{13} + V_{14} + V_{23} + V_{24}$, where V_{ij}, taken as a scalar-type interaction with a Gaussian shape, is

$$V_{ij} = -V_0 e^{-\beta^2|\vec{r}_i-\vec{r}_j|^2}(W + BP_{ij}^\sigma - MP_{ij}^\sigma P_{ij}^\tau - HP_{ij}^\tau), \tag{8}$$

and $\beta = 0.63$ F^{-1}. The exchange operator P_{ij}^σ (P_{ij}^τ) acts on the spin (isospin) variables of the nucleons i and

j. Because both Ψ_i and Ψ_f are antisymmetric under the exchange of nucleons 1 and 2, V_{1j} and V_{2j} have identical matrix elements. The transition matrix element T_{fi} is then

$$T_{fi} = 2[\Psi_f, (V_{13} + V_{14})\Psi_i]$$

$$= \text{const} \times \sum_{s\,m} (\tfrac{1}{2}\tfrac{1}{2}\bar{n}\,\bar{m}_4|sm) \sum_{j=3,4} I_j(s, \bar{\mu}_4\bar{\nu})\langle S^{\bar{\nu}}_{s\,m}(1, 2, 3; 4)\eta^{\bar{\mu}_4}_4\rho^{\bar{m}_5}_5\eta^{\bar{\mu}_5}_5, O_{1j}D^{M_d, 0}(1, 2)R^{n\,\nu}(3, 4, 5)\rangle , \tag{9}$$

where the spin wave function of the final-state interacting pair was expressed in its channel spin representation, i.e.,

$$R^{\bar{n}\,\bar{\nu}}(1, 2, 3)\rho^{\bar{m}_4}_4 = \sum_{s\,m} (\tfrac{1}{2}\tfrac{1}{2}\bar{n}\,\bar{m}_4|sm)S^{\bar{\nu}}_{s\,m}(1, 2, 3; 4) .$$

A bar was put on each final-state spin or isospin projection to distinguish it from that of the initial state. Operator O_{1j} is an abbreviation for the sum of operators, with $i=1$, in the parentheses of Eq. (8). Its matrix element $^{2s+1}\langle O_{1j}\rangle$ and the space integral I_j are calculated in the Appendix. The squared modulus of T_{fi}, averaged over the initial-state spin projections M_d and n and summed over the final-state spin projections $\bar{n}$, $\bar{m}_4$, and $\bar{m}_5$, becomes

$$\langle|T_{fi}|^2\rangle = \text{const} \times \sum_s \text{Tr}\left[\sum_{i=3,4} I_i(s, \bar{\mu}_4\bar{\nu})\,^{2s+1}\langle O_{1i}\rangle\right]\left[\sum_{j=3,4} I_j(s, \bar{\mu}_4\bar{\nu})\,^{2s+1}\langle O_{1j}\rangle\right]^\dagger .$$

In terms of the abbreviations defined as

$$^{2s+1}A = (W + M - \tfrac{1}{2}B - \tfrac{1}{2}H)I_3(s, \bar{\mu}_4\bar{\nu}) + (W - \tfrac{1}{2}H)I_4(s, \bar{\mu}_4\bar{\nu}) ,$$

$$^{2s+1}B = I_4(s, \bar{\mu}_4\bar{\nu})B ,$$

and

$$^{2s+1}C = -I_4(s, \bar{\mu}_4\bar{\nu})M ,$$

the final forms for $\langle|T_{fi}|^2\rangle$ are:

(1) For $D + {}^3\text{He} \to p + {}^3\text{He} + n$, i.e., $\bar{\mu}_4 = -\tfrac{1}{2}$ and $\bar{\nu} = \tfrac{1}{2}$,

$$\langle|T_{fi}|^2\rangle = K\left[\tfrac{1}{12}|{}^1A|^2 + \tfrac{1}{48}|{}^1B|^2 - \tfrac{1}{12}\text{Re}\,{}^1A{}^1B* + \tfrac{1}{4}|{}^3A|^2 + \tfrac{11}{48}|{}^3B|^2 + \tfrac{1}{3}|{}^3C|^2 + \text{Re}\left(\tfrac{5}{12}{}^3A{}^3B* + \tfrac{1}{2}{}^3B{}^3C* + \tfrac{1}{3}{}^3C{}^3A*\right)\right] . \tag{10a}$$

(2) For $D + {}^3\text{He} \to p + {}^3\text{H} + p$, i.e., $\bar{\mu}_4 = \tfrac{1}{2}$ and $\bar{\nu} = -\tfrac{1}{2}$,

$$\langle|T_{fi}|^2\rangle = K\left(\tfrac{1}{12}|{}^1A|^2 + \tfrac{1}{48}|{}^1B|^2 - \tfrac{1}{12}\text{Re}\,{}^1A{}^1B* + \tfrac{1}{4}|{}^3A|^2 + \tfrac{11}{48}|{}^3B|^2 + \tfrac{5}{12}\text{Re}\,{}^3A{}^3B*\right) . \tag{10b}$$

Here K is a numerical constant, independent of which one of the branches the reaction leads to. These expressions of $\langle|T_{fi}|^2\rangle$ were substituted into Eq. (7) for the calculation of differential cross sections.

IV. COMPARISON WITH DATA

As described in the Appendix, the ${}^3\text{He} + n$ or ${}^3\text{H} + p$ final-state interaction is taken into account by the factored-wave-function method in terms of the scattering-matrix amplitude D_{sl} and the phase shift δ_{nsl} or δ_{psl} given in the literature[9,10] (see Table I). For a range of nuclear forces[14] $a = 3.0$ F, a cutoff radius[5] $R_c = 5.0$ F, and Rosenfeld type of nucleon-nucleon interaction,[15] the calculated differential cross sections were compared by a least-squares fit with the angular correlations obtained at $E_p = 7.8$ MeV. The dashed curves shown in Fig. 5 represent the calculations from the D_{sl}, δ_{nsl}, and δ_{psl} given by Meyerhof and McElearney[10]; the solid curves are the same calculations except that

the triplet s-wave ${}^3\text{He} + n$ phase shift, i.e., δ_{n10}, was changed to that of Bransden, Robertson, and Swan.[9] For the partial waves other than the triplet s wave, the ${}^3\text{He} + n$ phase shifts of Meyerhof and McElearney[10] and Bransden, Robertson, and Swan[9] agree in signs. Although the values given by the latter are smaller, the data are unable to indicate any definite preference between the two. We used the values given by Bransden, Robertson, and Swan[9] for all of the $n + {}^3\text{He}$ phase shifts in the computations of the curves shown in Fig. 4. The same normalization constant, obtained from the least-squares fit for the angular correlations at $E_p = 7.8$ MeV, was used to calculate the differential cross sections for other proton energies.

As indicated in Table I, the phase shift δ_{n10} from

the resonating-group calculation of Bransden, Robertson, and Swan[9] is negative. The fact that our correlation data give a definite preference over this sign agrees with the results of Barit and Sergeev[11] in their analysis of the nucleon scattering by $A = 3$ nuclei. Since there is no 1^+ level below the ^{3}He + n threshold, the principle of charge invariance implies that δ_{n10} should vary approximately as δ_{p10}, which is negative according to Meyerhof and McElearney. With the D_{s0}, δ_{ns0}, and δ_{ps0} given in Ref. 11, and those D_{s1}, δ_{ns1}, and δ_{ps1} used in calculating the curves in Fig. 4, a similar fit to the data was obtained, but with a better prediction on the energy dependence of the p-^{3}H correlations.

The quality of the fit is found to be not sensitive to the cutoff radius R_c; the space integral I_4 is very much smaller than I_3 for R_c chosen to be somewhat greater than 2.0 F. The main contribution to T_{fi} comes from I_3; thus the constants of the nucleon-nucleon interaction appear effectively in $(W + M - \frac{1}{2}B - \frac{1}{2}H)^2$ as a common proportionality

factor. Since only the relative differential cross section was measured, the data cannot distinguish the difference in the choice of these constants in the nucleon-nucleon interaction. For lower proton energies, i.e., higher ^{4}He excitation energies, the agreement of calculations with the p-^{3}He angular correlations becomes poor; this may be due in part to the inappropriate p-wave ^{3}He + n phase shifts.

V. CONCLUSION

As in the recent investigations of the first excited state of ^{4}He via ^{7}Li(p, α) (Ref. 14), we have also found in D(^{3}He, p) a phase-space region in which the ^{3}He + n or ^{3}H + p final-state interaction is dominant. The anisotropy in the observed angular correlations indicates the importance of the p-wave final-state interactions. From the symmetry of the angular correlation and a modified-Born-approximation calculation, we believe that the ^{3}He stripping of its deuteron is a predominant mech-

TABLE I. A summary of the scattering-matrix amplitudes and the phase shifts used for comparison with the experimental data.

Partial wave	E_p (MeV)	E_x (MeV)	D_{sl} Ref. 10 [a]	δ_{psl} (rad) Ref. 10 [a]	δ_{psl} (rad) Ref. 9 [b]	δ_{nsl} (rad) Ref. 10 [a]	δ_{nsl} (rad) Ref. 9 [b]
^1S	8.6	20.622	0.77	1.75	−0.17	−0.30	−0.04 [a, b]
	8.2	20.952	0.66	1.70	−0.22	−0.60	−0.12
	7.8	21.236	0.63	1.65	−0.26	−0.70	−0.20
	7.4	21.515	0.62	1.60	−0.32	−0.82	−0.26
	7.0	21.788	0.62	1.58	−0.34	−0.90	−0.30
	6.6	22.055	0.62	1.56	−0.37	−0.98	−0.33
^3S	8.6	20.622	0.94	−0.44	−0.39	0.22	−0.10
	8.2	20.952	0.85	−0.50	−0.48	0.50	−0.31
	7.8	21.236	0.77	−0.60	−0.56	0.67	−0.47
	7.4	21.515	0.72	−0.65	−0.63	0.85	−0.57
	7.0	21.788	0.67	−0.75	−0.70	1.10	−0.65
	6.6	22.055	0.62	−0.85	−0.75	1.35	−0.72
^1P	8.6	20.622	0.99	0.16	−0.02	−0.01	−0.00
	8.2	20.952	0.96	0.34	−0.03	−0.05	−0.01
	7.8	21.236	0.90	0.42	−0.04	−0.10	−0.02
	7.4	21.515	0.78	0.50	−0.05	−0.15	−0.03
	7.0	21.788	0.68	0.63	−0.06	−0.32	−0.04
	6.6	22.055	0.57	0.76	−0.07	−0.49	−0.05
^3P	8.6	20.622	1.00	0.18	0.07	0.01	0.00
	8.2	20.952	1.00	0.36	0.14	0.08	0.05
	7.8	21.236	1.00	0.40	0.21	0.13	0.10
	7.4	21.515	1.00	0.53	0.28	0.20	0.17
	7.0	21.788	1.00	0.68	0.36	0.30	0.23
	6.6	22.050	1.00	0.83	0.41	0.40	0.32

[a] See Ref. 10. The region of validity is $E_x \lesssim 21.3$ MeV; D_{sl}, δ_{psl}, and δ_{nsl}, for $E_x > 21.3$ MeV, are obtained by extrapolations.

[b] See Ref. 9. The inelasticity was not considered; thus $D_{sl} = 1$ for all energies. The values for D_{sl} given in Ref. 10 were assumed in calculations of p-^{3}He correlations. The phase shifts listed are the averages of those derived from the Serber force and from the symmetrical force.
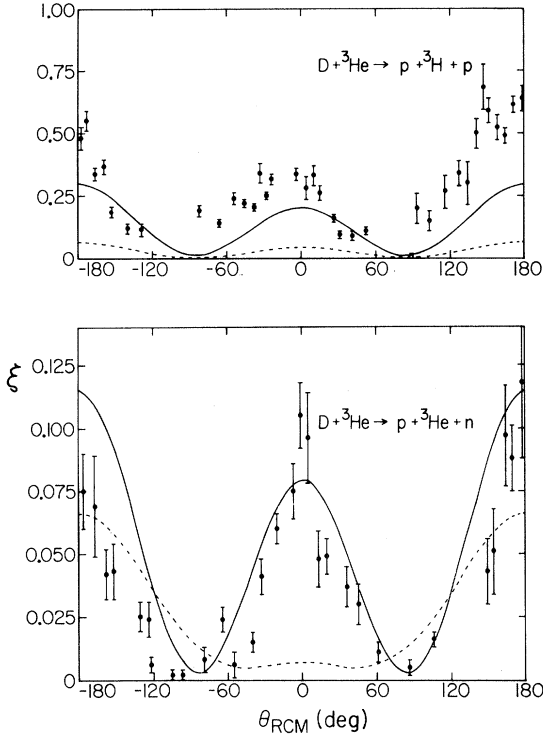
FIG. 5. Least-squares fit to the angular correlations obtained at $E_p = 7.8$ MeV (see also Fig. 4) were fitted with the modified-Born-approximation calculations. The dashed curves represent the results using all the scattering-matrix amplitudes and phase shifts given by Meyerhof and McElearney. The fits, especially to the shape of the p-^{3}He angular correlations and the branching ratio of the two modes of the reaction, were poor. The solid curves are the result of the same calculation except that the ^3S phase shifts for $n + {}^3$He were replaced by the values of Bransden, Robertson, and Swan.

anism, at least in the phase-space region covered by this experiment. The charge-exchange processes[16] were not considered here; it may become important if the protons are detected in backward directions. The factored-wave-function approach is useful to take into account the final-state interactions for $E_x \leqslant 21.6$ MeV. In order to say whether the method is still applicable for higher ^{4}He excitation energies, it is clear that one needs to have a better knowledge about the excited ^{4}He system; in particular, the p-wave ^{3}He $+ n$ phase shifts.

ACKNOWLEDGMENTS

APPENDIX

Explicitly the matrix $\langle O_{1j} \rangle$, defined in Eq. (9), is related to the direct and exchange spin-isospin overlaps as

$$\langle O_{1j} \rangle = W \langle 1 \rangle - M \langle P_{1j}^\sigma P_{1j}^\tau \rangle + B \langle P_{1j}^\sigma \rangle - H \langle P_{1j}^\tau \rangle \;.$$

Because of symmetry properties of the spin-isospin wave functions, it was found that

$$\langle P_{13}^\sigma \rangle = -\tfrac{1}{2}\langle 1 \rangle, \quad \langle P_{13}^\tau \rangle = \tfrac{1}{2}\langle 1 \rangle, \quad \langle P_{13}^\sigma P_{13}^\tau \rangle = -\langle 1 \rangle,$$

and

$$\langle P_{14}^\tau \rangle = \tfrac{1}{2}\langle 1 \rangle \;.$$

Evaluations of $\langle 1 \rangle$, $\langle P_{14}^\sigma \rangle$, and $\langle P_{14}^\sigma P_{14}^\tau \rangle$ involve systematic bookkeeping of the Clebsch-Gordan coefficients and of the Kronecker δ functions, which come in directly from the orthogonal properties of the spin and isospin matrices. In terms of a 2×2 matrix,

$$X_{a,b} = \sum_\sigma (\tfrac{1}{2}\tfrac{1}{2}\sigma a | 1 M_d)(\tfrac{1}{2}\tfrac{1}{2}\sigma b | sm) \;,$$

where $M_d(m)$ is the spin projection of the initial-state deuteron (final-state ^{4}He system), the matrix elements can be expressed as

$$\langle 1 \rangle = -\frac{1}{6\sqrt{2}} \, \delta_{\overline{m}_5,n} \, \delta_{s,1} \delta_{m,M_d} - \tfrac{1}{6}(\tfrac{1}{2}\,\tfrac{1}{2}\,\overline{\mu}_4\overline{\nu}|00)[\delta_{\overline{m}_5,n}(X_{-n,-n} - X_{n,n}) + 2\delta_{\overline{m}_5,-n}X_{-n,n}] \;,$$

$$\langle P_{14}^\sigma \rangle = -\frac{1}{4\sqrt{2}} \, \delta_{\overline{m}_5,n} \delta_{s,1} \delta_{m,M_d} - \frac{(-)^{s+1}}{12}(\tfrac{1}{2}\,\tfrac{1}{2}\,\overline{\mu}_4\overline{\nu}|00)[\delta_{\overline{m}_5,n}(X_{-n,-n} - X_{n,n}) + 2\delta_{\overline{m}_5,-n}X_{-n,n}] \;,$$

and

$$\langle P_{14}^\sigma P_{14}^\tau \rangle = \tfrac{1}{6}\delta_{\overline{m}_5,n}\left[-\frac{1}{\sqrt{2}}\,\delta_{s,1}\delta_{m,M_d} + (-)^{s+1}(\tfrac{1}{2}\,\tfrac{1}{2}\,\overline{\mu}_4\overline{\nu}|00)(X_{-n,-n} + X_{n,n}) \right] \;.$$

Here $n(\overline{m}_5)$ is the spin projection of the initial-state ^{3}He (final-state proton). Depending on the channel spin s and on the type of the final-state interacting pair, the numerical values of those $6 \times [2(2s+1)]$ matrices can be found easily, and were used in the derivation of Eqs. (10a) and (10b).

The space integral I_j for $j = 3$ or 4, defined as

$$I_j = 5 \int \exp\{-i\vec{K}_p \cdot [\vec{r}_5 - \tfrac{1}{4}(\vec{r}_1 + \vec{r}_2 + \vec{r}_3 + \vec{r}_4)]\} \exp\{-\gamma^2[\tfrac{3}{4}|\vec{r}_1 - \vec{r}_2|^2 + |\vec{r}_3 - \tfrac{1}{2}(\vec{r}_1 + \vec{r}_2)|^2]\}$$

$$\times \chi_4'^*[\vec{r}_4 - \tfrac{1}{3}(\vec{r}_1 + \vec{r}_2 + \vec{r}_3)] \, e^{-\beta^2|\vec{r}_1 - \vec{r}_j|^2} \exp\{i\vec{K}_T \cdot [\tfrac{1}{3}(\vec{r}_3 + \vec{r}_4 + \vec{r}_5) - \tfrac{1}{2}(\vec{r}_1 + \vec{r}_2)]\}$$

$$\times e^{-\alpha^2|\vec{r}_1 - \vec{r}_2|^2} \exp\{-\gamma^2[\tfrac{3}{4}|\vec{r}_3 - \vec{r}_4|^2 - |\vec{r}_5 - \tfrac{1}{2}(\vec{r}_3 + \vec{r}_4)|^2]\} d\vec{r}_1 d\vec{r}_2 d\vec{r}_3 d\vec{r}_4 ,$$

were first simplified by using a new set of integration variables, $\vec{y}_1 = \vec{r}_1 - \vec{r}_2$, $\vec{y}_2 = \vec{r}_5 - \tfrac{1}{2}(\vec{r}_3 + \vec{r}_4)$, $\vec{y}_3 = \vec{r}_3 - \tfrac{1}{2}(\vec{r}_1 + \vec{r}_2)$, and $\vec{\rho} = \vec{r}_4 - \tfrac{1}{3}(\vec{r}_1 + \vec{r}_2 + \vec{r}_3)$. The $\vec{y}_1$ and $\vec{y}_2$ integrations are separable and can be carried out analytically. To separate the last two integrations, a further transformation was made. If one writes $\vec{z} = \vec{y}_3 + f_j \vec{\rho}$ and properly chooses f_j such that the coefficients of $\vec{z} \cdot \vec{\rho}$ in the exponent vanish, the final result of I_j is given by

$$I_j = 8\pi^3 [\gamma^2 (4\alpha^2 + 3\gamma^2 + \beta^2)]^{-3/2} \left(\frac{\pi}{\zeta^2 b_j^2 + \tfrac{4}{3}\gamma^2}\right)^{3/2} \exp(-|\tfrac{1}{3}\vec{K}_T - \vec{K}_p|^2/4\gamma^2)$$

$$\times \exp[-|\tfrac{2}{3}\vec{K}_T + \tfrac{1}{3}\vec{K}_p|^2/4(\zeta^2 b_j^2 + \tfrac{4}{3}\gamma^2)] \int \chi_4'^*(\vec{\rho}) e^{-\xi_j^2 \rho^2} e^{i\vec{P}_j \cdot \vec{\rho}} d\vec{\rho} ,$$

where

$$\zeta^2 = \beta^2 (4\alpha^2 + 3\gamma^2)/(4\alpha^2 + 3\gamma^2 + \beta^2), \quad f_j = (2\zeta^2 a_j b_j - \gamma^2)/(\tfrac{8}{3}\gamma^2 + 2\zeta^2 b_j^2),$$

$$\xi_j^2 = (\zeta^2 b_j^2 + \tfrac{4}{3}\gamma^2)f_j^2 + (\gamma^2 - 2a_j b_j \zeta^2)f_j + (\zeta^2 a_j^2 + \tfrac{3}{4}\gamma^2), \quad \vec{P}_j = (\tfrac{4}{3}f_j - 1)(\tfrac{1}{4}\vec{K}_p - \tfrac{1}{2}\vec{K}_T),$$

and a_3 (a_4) and b_3 (b_4) are, respectively, equal to 0 (-1) and -1 ($-\tfrac{1}{3}$). The angular part of the $\vec{\rho}$ integration can be done by expanding $\chi_4'(\vec{\rho})$ and $e^{i\vec{P}_j \cdot \vec{\rho}}$ into partial waves. That is,

$$\int \chi_4'^*(\vec{\rho}) e^{-\xi_j^2 \rho^2} e^{i\vec{P}_j \cdot \vec{\rho}} d\vec{\rho} = \frac{2\pi}{k} e^{i\sigma_0} \sum_l (2l+1) P_l(\hat{P}_j \cdot \hat{k}) \int_0^\infty U_l^*(k\rho) j_l(P_j \rho) e^{-\xi_j^2 \rho^2} \rho \, d\rho ,$$

where $\hbar\vec{K}$ is the relative momentum of the final-state interacting pair of particles, and σ_0 is the s-wave Coulomb phase shift. The function $U_l(k\rho)$, which becomes $I_l(k\rho) - D_{sl} e^{2i\delta_{sl}} O_l(k\rho)$ for ρ greater than the range of nuclear force a, is the radial wave function of the final-state interacting pair of particles. In accordance with the factored-wave-function method,[5,6] the integral over ρ was approximated as

$$\int_0^\infty U_l^*(k\rho) j_l(P_j \rho) e^{-\xi_j^2 \rho^2} \rho \, d\rho \approx [O_l(ka) - D_{sl} e^{-2i\delta_{sl}} I_l(ka)] \int_{R_c}^\infty j_l(P_j \rho) e^{-\xi_j^2 \rho^2} \rho \, d\rho ,$$

where a cutoff radius R_c was introduced to simulate the distort effects[5] in the reaction.

---

[1]P. G. Young and G. G. Ohlsen, Phys. Letters **8**, 124 (1964).

[2]P. D. Parker, P. F. Donovan, J. V. Kane, and J. F. Mollenauer, Phys. Rev. Letters **14**, 15 (1965).

[3]R. W. Zurmühle, Nucl. Phys. **72**, 225 (1965).

[4]W. E. Meyerhof, Rev. Mod. Phys. **37**, 512 (1965).

[5]D. U. L. Yu and W. E. Meyerhof, Nucl. Phys. **80**, 481 (1966).

[6]C. Werntz, Phys. Rev. **128**, 1336 (1962).

[7]H. W. Lefevre, R. R. Borchers, and C. H. Poppe, Phys. Rev. **128**, 1328 (1962).

[8]C. H. Poppe, C. H. Holbrow, and R. R. Borchers, Phys. Rev. **129**, 733 (1963).

[9]H. Bransden, H. H. Robertson, and P. Swan, Proc. Phys. Soc. (London) **A69**, 877 (1956).

[10]W. E. Meyerhof and J. N. McElearney, Nucl. Phys. **74**, 533 (1965).

[11]I. Ya. Barit and V. A. Sergeev, Yadern. Fiz. **4**, 712 (1966) [transl.: Soviet J. Nucl. Phys. **4**, 507 (1967)].

[12]The relative amplitude calculated is the product $n_i I_i \exp(K_i^2/4A_i^2) J_{l,i}$ according to Eqs. (24a), (24b), and (24c) in Ref. 5, where cutoff radii R_1 and R were both chosen to be 5 F.

[13]L. I. Schiff, Phys. Rev. **133**, B802 (1964).

[14]W. K. Lin, F. Scheibling, and R. W. Kavanagh, Phys. Rev. C **1**, 816 (1970).

[15]M. A. Preston, *Physics of the Nucleus* (Addison-Wesley Publishing Company, Inc., Reading, Massachusetts, 1962), p. 179.

[16]E. M. Henley and F. C. Richards, Nucl. Phys. **A103**, 361 (1967).